Pilot fuel injection optimization in an annular combustor.

P. Di Martino, G. Cinque & A. Terlizzi.

1. Fiat Avio S.p.A., Pomgliano d'Arco (Naples), Italy

Abstract
In the last decades Computation Fluid Dynamics (CFD) tools have turned out to be very effective to accelerate the development of combustor design. The high degree of reliability achieved by numerical methods in the prediction of combustion phenomena would expect to reduce the number of configurations to be manufactured and tested, when improved performances are required to a combustion system.
In the framework of a research programme (LOPOCOTEP) funded by EC, CFD activities were carried out by FIAT AVIO Pomigliano, aimed to the design optimization of a reverse flow annular combustor for small engines. A significant reduction of pollutant emissions, namely nitrogen oxides, has been obtained. Several configurations with different air splits and pilot injection angles were analyzed at take-off conditions. The assessment was made on the basis of global parameters (OTDF, RTDF, emission indexes) and distribution of temperatures in some specific planes.

1. Introduction

This paper deals with the optimization of annular combustor of the reverse flow type equipped with lean premixed prevaporized (LPP) ducts in order to reduce the NO_x emissions.
A previous configuration of the combustor was designed and manufactured in the European Project BRITE LN3.
During the experimental tests performed at Fiat Avio Naples and at ONERA in Paris, high values of NO_x emissions index as well as high values of liner wall temperatures have been measured. For that reason it was decided to modify the combustor geometry and the airsplit. A new impingement cooling device was designed and extensive CFD analyses have been carried out to find out the pilot injection configuration that gives the minimum nitrogen oxide emission index.
On one hand the split of air was changed, increasing the mass flow rate through the premixing ducts, on the other one the geometry of the pilot was modified, optimizing the injection angles respect to the radial and tangential direction. A pilot configuration with two injection points was numerically tested too. This choice affects the liquid injection strategies, since different types of atomizer and/or different atomizer adjustments have to be selected to create better fuel-air mixing conditions. Therefore this work represents the first step in an inverse design approach for the integration of the fuel spray in the whole gas turbine configuration.

2. Gas-phase governing equations

Fiat Avio in-house code BODY3D was used for reactive CFD analyses. In that code steady fully elliptic density-weighted Navier-Stokes (NS) equations describing gas phase, under low Mach number approximation, coupled to the energy and momentum balance equations for the

liquid phase, are considered [1]. Turbulence is simulated by way of the standard k-ε, model along with the wall function treatment for the near-wall regions. The conservation equations solved for the gas phase are those for momentum, mass, kinetic energy of turbulence and its dissipation, energy and chemical species.
In order to fit the very complex geometries encountered in industrial applications, a body conforming system of coordinates is used. Therefore it is necessary to transform the NS equations from Cartesian coordinates (x,y,z) to curvilinear non-orthogonal coordinates (ξ,η,ζ). The final equations to be solved are [2]:

$$\frac{\partial}{\partial\xi}(\rho U\phi)+\frac{\partial}{\partial\eta}(\rho V\phi)+\frac{\partial}{\partial\zeta}(\rho W\phi)=\frac{\partial}{\partial\xi}\left(\frac{\Gamma_\phi}{J}q_{11}\frac{\partial\phi}{\partial\xi}\right)+\frac{\partial}{\partial\eta}\left(\frac{\Gamma_\phi}{J}q_{22}\frac{\partial\phi}{\partial\eta}\right)+\frac{\partial}{\partial\zeta}\left(\frac{\Gamma_\phi}{J}q_{33}\frac{\partial\phi}{\partial\zeta}\right)+$$
$$\frac{\partial}{\partial\xi}\left[\frac{\Gamma_\phi}{J}\left(q_{12}\frac{\partial\phi}{\partial\eta}+q_{13}\frac{\partial\phi}{\partial\zeta}\right)\right]+\frac{\partial}{\partial\eta}\left[\frac{\Gamma_\phi}{J}\left(q_{21}\frac{\partial\phi}{\partial\xi}+q_{23}\frac{\partial\phi}{\partial\zeta}\right)\right]+\frac{\partial}{\partial\zeta}\left[\frac{\Gamma_\phi}{J}\left(q_{31}\frac{\partial\phi}{\partial\xi}+q_{32}\frac{\partial\phi}{\partial\eta}\right)\right]+ \quad (1)$$
$$J\cdot(S_g(\xi,\eta,\zeta)+S_d(\xi,\eta,\zeta))$$

In the foregoing mathematical expression U,V,W are the so-called contravariant velocity components, J is the Jacobian of the coordinate transformation, q_{ij} are metric quantities; terms with $i\neq j$ account for grid distortion.
All terms which arise in addition to convection and diffusion are grouped in the source-term S_g for the gas-phase, while S_d accounts for liquid droplets.
Turbulence is simulated by way of the standard k-ε model along with the wall function treatment for the near-wall regions.
There are several approaches for modelling the combustion in turbulent flows. In this study we have chosen the model based on Arrhenius and Eddy Break Up [3] concepts.
The heat release model is given by the following two-step scheme, which allows for calculation of CO (finite rate kinetics):

$$C_xH_y+(0.5x+0.25y)O_2\rightarrow xCO+0.5yH_2O \qquad CO+0.5O_2\rightarrow CO_2 \quad (2)$$

The density is provided by the law of perfect gases while temperature is updated from stagnation enthalpy.

3. Liquid-phase model

The behaviour of fuel droplets and the rate at which they evaporate in the premixing zone of a combustion chamber is very important as this dictates the level of homogeneity achieved in mixing the fuel and air, which directly controls the levels of NO_x produced. To model the droplet transport and evaporation rates correctly, suitable interphase interactions for mass, momentum and energy need to be implemented in Computational Fluid Dynamic (CFD) codes. Among the several spray models available in literature [4] we have chosen the deterministic separated flow model (DSF).
This model assumes that the fuel is injected into the combustion chamber as a fully atomized spray, which consists of spherical droplets. Finite interphase transport rates are considered, but the effects of turbulent fluctuations on particle motion are neglected. According to some authors [5] the gas phase heat and mass transfer may be considered as quasi steady. The pressure drop in the gas is negligible and the thermophysical properties of the air-vapor

mixture may be treated as constants, provided they are evaluated at reference temperature and composition ("1/3" rule). Droplets are assumed to interact only with the mean gas motion. Particles follows deterministic trajectories found by solving their Lagrangian equations of motion. The model takes into account drop heat-up, including the effect of forced convection. The evaporated mass flux is based on the vapor concentration gradient concept that estimates the gas properties at the above reference temperature. Besides the infinite conductivity hypothesis [5] is used to calculate drop temperature for a Lewis number of unity.
The liquid-phase equations are coupled to the equations describing gas-phase through the droplet source terms, which are obtained by calculating what is lost or gained in terms of mass; momentum and energy as the droplets enter and leave volume elements. The set of simultaneous ordinary equations for liquid phase is solved by the fourth order Runge-Kutta method at suitable intervals within the iterative procedure. The time step is dynamically adjusted based on droplet velocity and grid cell size. The equations describing the liquid phase are:

$$\frac{dT_F}{dt} = \frac{\dot{m}_F L}{Cp_F \cdot m_F}\left(\frac{B_T}{B_M} - 1\right) \tag{3}$$

$$\frac{dD}{dt} = -\frac{4 \cdot k_g \cdot (Log_e(1 + B_M)) \cdot (2 + 0.6\,Re^{0.5} Pr^{0.33})}{\rho_F \cdot Cp_g \cdot D} \tag{4}$$

$$m_F = \frac{\pi}{6}\rho_F D^3 \;\; ; \;\; \dot{m}_F = 2\pi D \cdot \left(\frac{k}{Cp}\right)_g \cdot Log_e(1 + B_M) \tag{5}$$

$$B_M = \frac{Y_{F_S}}{1 - Y_{F_S}} \;\; ; \;\; B_T = \frac{Cp_g \cdot (T_{GAS} - T_F)}{L} \tag{6}$$

4. NO_x modelling

There are three separate routes to NO production: thermal, prompt and nitrous-oxide mechanism. As we work under lean premixed conditions, the flame temperature is reduced and prompt route dominates with respect the thermal NO_x mechanism. The nitrous oxide route is also important in this case [8]. The rates of prompt NO and nitrous oxide have been empirically derived using a low activation energy. The extended Zeldovitch mechanism has been considered for the thermal NO formation. The NO_x model has been validated by comparison with experiments carried out at ONERA.

5. Combustor description

The annular combustor included 14 premixing ducts (LPP) and 7 pilot injectors for the stabilization of the flame (Fig. 1).

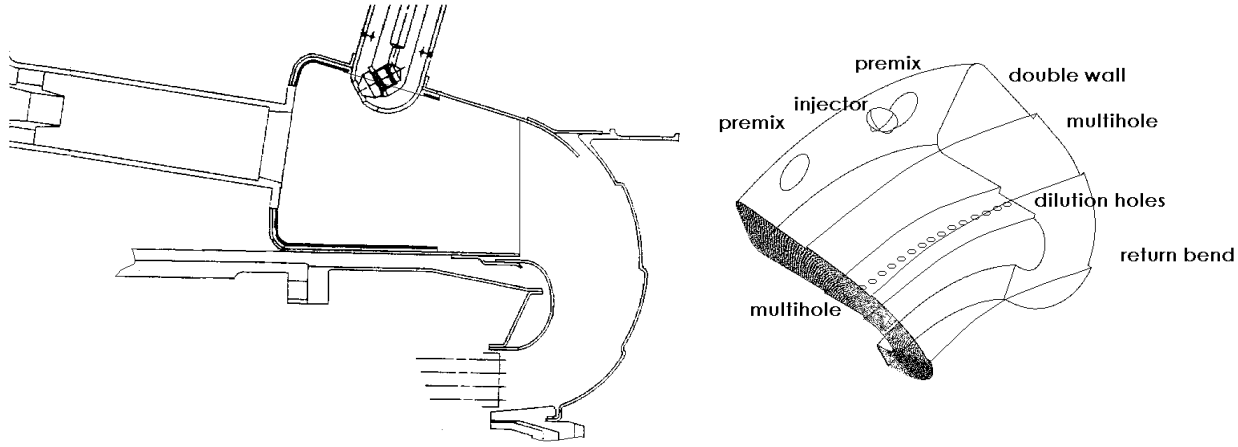

Fig. 1 Schematic of annular combustor.

The computational domain was a combustor sector including 2 LPP ducts with one pilot and periodic boundary conditions at both side view planes. A structured mesh (Fig. 2) with blocked cells was used for the calculations with about 600,000 cells.

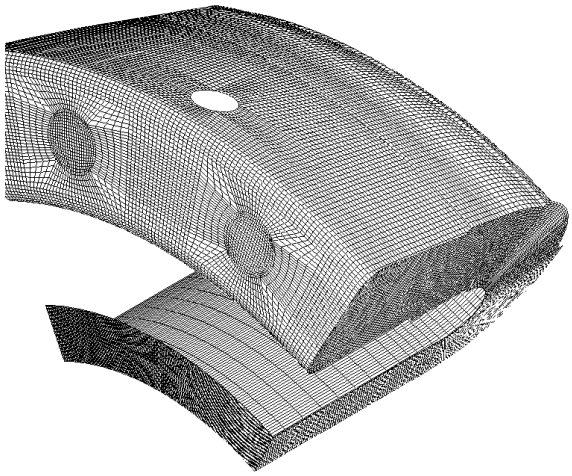

Fig. 2 Three-dimensional view of the model grid mesh.

The boundary conditions at exit of LPP ducts were taken from distributions of velocity components, turbulence parameters and mixture fraction results of previous calculation on the ducts alone.

The liquid droplets were injected on a hollow cone with fixed opening angle and initial velocity. A Rosin-Rammler distribution for droplet diameters with a SMD (Sauter mean diameter) of 20 μm was used.

Different pilot injection configuration have been analyzed (Fig. 3): one injection point with radial angle of 55º and 40º and tangential angle of 25º; double injection point with the same angles and double injection point with tangential angle of 0º.

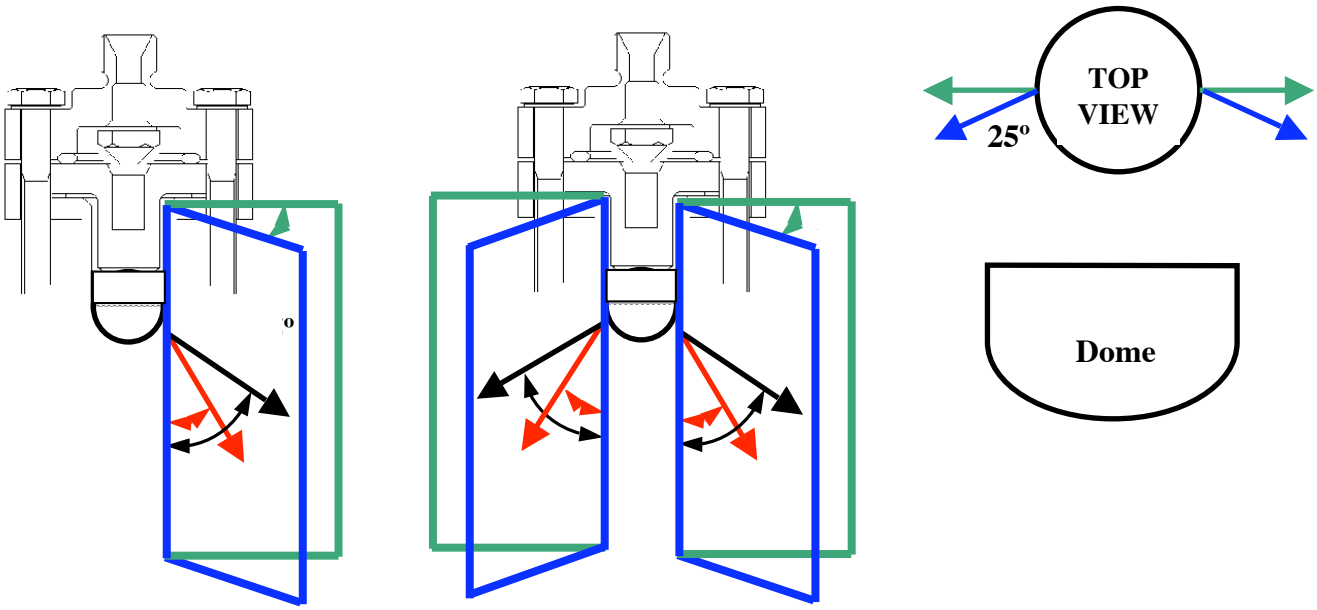

Fig. 3 Different injection systems: single and double injection point.

6. Optimization activity

The starting point is: high level of nitrogen oxide emission and high wall temperature occurred during the ONERA tests. Consequently different air splits have been defined in order to get better values of pollutant emissions. In the following Table 1 are summarized the main variations with respect to the original air split. The rest of air percentage for the other devices is not mentioned because such data are considered confidential.

Table 1 Different air splits for combustor devices (%).

	Original air split	Modified air split	New air split
Premix duct	26.1	30.1	30
Dilution holes	15.5	7.5	7
DBL Outer	4.3	4.3	11.05

7. Discussion of results

Along with the different air splits, several pilot injection systems have been chosen: single pilot injection with initial angle (55º), double pilot injection with initial angle (55º), double

pilot injection with modified angle (40º). All these injection configurations have a tangential angle of 25º with respect to the normal to combustor axis. A final injection configuration considers double pilot injection with a tangential angle of 0º.
The following Table 2 illustrates the main results of optimization process.

Table 2 Matrix of results for different numerical tests.

Test condition	OTDF	RTDF	EI_NOx	EI_CO	EI_UHC
1			22.7	0.0165	2.87E-03
11	15.3	5.34	11.4	0.116	4.17E-02
14	17.7	6.5	8.83	1.16E-01	2.07E-02
15	19.2	6.13	8.57	0.142	2.55E-02
11A	17.4	4.71	12.3	4.69E-02	8.31E-03
14A	16.2	7.28	9.09	1.41E-01	4.52E-02
15A	19	6.57	8.83	1.57E-01	4.81E-02
11B	17.9	6.17	11.3	9.75E-02	3.68E-02
14B	22.8	5.43	7.97	1.22E-01	4.12E-02
15B	18.6	10.2	8.24	0.145	4.49E-02

Test condition No 1 is concerned with the experimental results obtained at ONERA with the original air split. Test conditions No 11, 14, 15 are concerned with the modified air split with single pilot (11), double pilot (14) and double pilot (15) with modified angle (40º instead of 55º) respectively. In all cases the injection tangential angle is 25º. We can note that there is a remarkable decrease of nitrogen oxide emission index moving from test No 11 to test No 15. The change form original air split to the modified air split adjusted the pollutant emission but wall temperatures remain still high. This is the reason why we tried a new air split. Test conditions No 11A, 14A, 15A refer to the new air split with single pilot (11A), double pilot (14a) and double pilot (15A) with modified angle (40º instead of 55º) respectively. In all cases the injection tangential angle is 25º. As it can be noted, we have an increase of nitrogen oxide emission index if we compare it to the previous air split. Better results have been obtained in terms of wall temperature.
In the final iteration we tried to find a balance between two opposite trends: nitrogen oxide emission index and wall temperature. Test conditions No 11B, 14B, 15B are concerned with the new air split with single pilot (11), double pilot (14) and double pilot (15) with modified angle (40º instead of 55º) respectively. Now the injection tangential angle is 0º. Finally we reached a good result because nitrogen oxide emission index were on the level of the modified air split but wall temperatures have been decreased. The effect of double injection system can be seen in Fig. 4, where the temperature fields at pilot injector cross planes are shown.

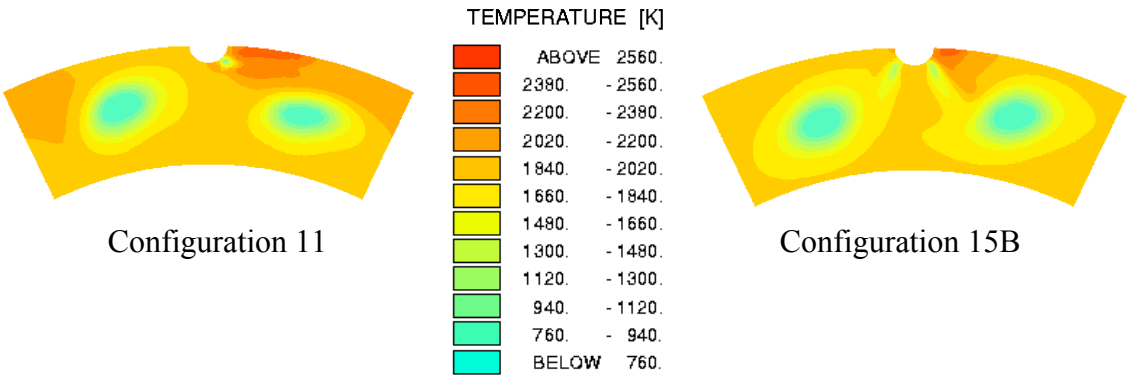

Fig. 4 Comparison of gas temperature in the injector cross plane.

As an example of wall temperatures we can look at Fig. 5, where a comparison between two configuration is shown.

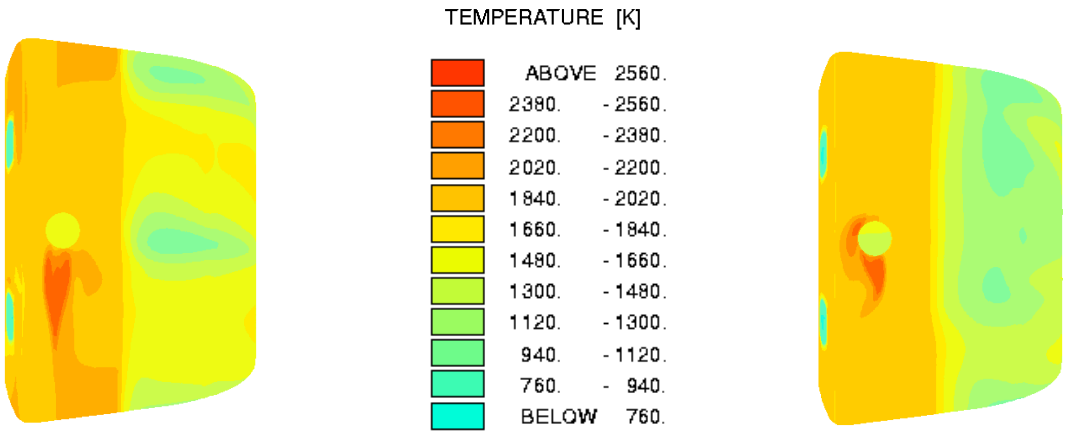

Fig. 4 Comparison wall temperature at the outer liner.

8. Final remarks

An optimization analysis has been carried out by means of an in-house CFD code in the framework of a research programme. The object of investigation has been an annular reverse flow combustor that was previously tested by ONERA. The experiments revealed too high wall temperature and unacceptable nitrogen oxides emission index. Consequently different air splits in conjunction with several configurations of pilot injection system have been analyze to achieve the best compromise between low pollutant emission index and reasonable wall temperatures. The air split has been done by modifying the hole number and diameter. The first air split aimed at improving the nitrogen oxide emission index. For this reason the mass flow rates through the premix duct and through the dilution holes were changed with respect to the original air distribution. The second air split allowed the dome cooling to be improved, lowering wall temperatures. Another key point was the selection of a double point pilot injection system with proper angles that optimized both nitrogen oxides and wall temperature. Configuration No 15B has been selected and it will be manufactured in the following of the project.

9. Acknowledgments

This work was supported by the European LOPOCOTEP research Project, Contract GRD1-2000-25062. The authors would like to thank all people who gave their contribution for helpful discussion and assistance with the experimental work.

10. References

[1] Gupta, A. K., and Lilley, D. G., Flowfield Modeling and Diagnostic, Abacus Press, 1985.

[2] Burns, A. D., Wilkes, N. S., A Finite Difference Method for the Computation of Fluid Flows on Complex Geometries, AERE-R 12342, Harwell Laboratory, Oxfordshire, U.K., 1987.

[3] Jones, W. P., Whitelaw, J. H., Calculation Methods for Turbulent Reacting Flows: a Review, Comb. Flame, Vol. 48, 1982, pp. 1-26.

[4] Aggarwal, S. K., Tong, A. Y., and Sirignano, W. A. "A Comparison of Vaporization Models in Spray Calculations", AIAA Journal, Vol. 22, No. 10, 1984, pp. 1448-1457.

[6] Hubbard, G. L., Denny, V. E., and Mills, A. F., "Droplet Vaporization: Effects of Transient and Variable Properties", Int. J. Heat Mass Transfer, Vol. 18, 1975, pp. 1003-1008.

[7] Faeth, G. M., "Evaporation and Combustion of Sprays", Prog. Energy Comb. Sci., Vol. 9, 1983, pp. 1-76.

[8] G. De Soete: “Overall Reaction Rates of NO and NO_2 Formation from Fuel Nitrogen”, Int. 15th Symp on Combustion, 1974 , p. 1093, The Combustion Institute.